Temperature and electric field tuning of the ferroelectric soft mode in a strained SrTiO₃/DyScO₃ heterostructure

C. Kadlec,[1] V. Skoromets,[1] F. Kadlec,[1] H. Němec,[1] J. Hlinka,[1] J. Schubert,[2] G. Panaitov,[2] and P. Kužel[1],*

[1]*Institute of Physics, Academy of Sciences of the Czech Republic, Na Slovance 2, 182 21 Prague 8, Czech Republic*
[2]*Institute of Bio and Nanosystems, Research Centre Jülich, JARA–Fundamentals of Future Information Technology, D-52425 Jülich, Germany*

We studied THz dielectric spectra of SrTiO₃/DyScO₃ epitaxial multilayers with four 50-nm-thick layers of each compound deposited on DyScO₃ substrate as a function of temperature and electric field. At room temperature, SrTiO₃ is in the paraelectric phase and, due to the in-plane tensile strain within the films, the soft-mode frequency is shifted down to 47 cm^{-1}. The ferroelectric phase transition occurs in the strained SrTiO₃ layers around 270 K and in the ferroelectric phase the soft-mode hardening upon temperature decrease is observed. The soft mode is linearly coupled to an excitation of relaxation type at 10 cm^{-1} at all temperatures. This relaxation is silent in the paraelectric phase, but it becomes coupled to the polarization below the ferroelectric transition temperature and its strength progressively increases. The recently proposed universal model of soft-mode behavior in strained SrTiO₃ films [C. Kadlec *et al.*, J. Phys.: Condens. Matter **21**, 115902 (2009)] was generalized to describe the observed spectra at all temperatures and applied fields.

I. INTRODUCTION

Research on dielectric properties of materials in the terahertz spectral range gains importance both for understanding the fundamental processes with spectral signatures in the far infrared and for the development of new applications in the terahertz technology.[1]

Switchable and tunable structures operating in the terahertz range are currently of high interest for the THz technology with possible applications in future short-range wireless communications.[2] Various metallic and/or semiconductor metamaterial and photonic structures were proposed to achieve these aims.[3–6] Electric field tunable dielectrics constitute another class of materials, which may play a significant role in this research.[7–9]

In ferroelectrics, dispersion and absorption related to the ferroelectric soft-mode frequently appear in the upper part of the terahertz range; in addition (or alternatively), a relaxation behavior due to polar disorder is observed in its lower part. These excitations play the key role in the low-frequency dynamics and usually drive the ferroelectric phase transition in these compounds.[10]

Strontium titanate (SrTiO₃, STO) is an incipient ferroelectric showing a strong ferroelectric soft mode. In other ferroelectric compounds with perovskite structure, such as BaTiO₃, the frequency of the soft phonon mode decreases with temperature in the paraelectric phase to give rise of the ferroelectric phase transition. The ferroelectric transition does not occur in STO single crystals due to quantum fluctuations at low temperatures.[11] Recently, it has been reported that very thin STO films may exhibit the ferroelectric phase transition provided they are deposited on substrates, showing a suitable lattice-parameter mismatch with STO in order to induce an in-plane tensile strain within the STO film.[12] The phase transition appears close to room temperature in these films for the lattice mismatch of about 1%, which can be achieved, e.g., on (110) DyScO₃ (DSO) substrates.[13] Such

layers show an enhanced tunability of the complex microwave and terahertz dielectric function at room temperature as compared to single crystals and unstrained films.[14–16]

It has been demonstrated that STO/DSO multilayers can be grown on DSO substrates with the aim to increase the total thickness of the strained STO.[7,16] A strong strain and, as a consequence, high values of the subterahertz dielectric function at room temperature can then be maintained across at least 200 nm of the total thickness of STO layers.[16]

Recently, a new mode of relaxation type (central mode) has been observed in strained STO films and STO/DSO multilayers.[7,17] The origin of the coexistence of a soft and central modes close to phase transitions in many perovskite ferroelectrics is still under debate. Recently, an *ab initio* modeling supported by THz experimental data has demonstrated its close relation to the anharmonicity of the soft-mode potential in the ferroelectric BaTiO₃.[18,19]

In this paper, we report on a study of THz dielectric properties and field-induced tunability of strained STO multilayer in a temperature range of 20–300 K, which encompasses the ferroelectric phase transition. The character of the coupling of the previously reported[7,16] low-frequency relaxation mode is deduced from low-temperature data.

II. EXPERIMENTAL DETAILS

We investigated the temperature-dependent dielectric properties of a multilayer sample (denoted below as 4×50A) consisting of four STO/DSO bilayers deposited on a DSO single-crystal substrate, which was previously studied at room temperature in Ref. 7; details on the substrate and multilayer preparation are provided therein. The multilayer was prepared by pulsed laser deposition technique and, subsequently, an interdigitated gold electrode structure was deposited on the top STO layer such that it covered about one half of the 1 cm² sample surface. For comparison, and in order to check the accuracy of the temperature-dependent

measurements, another (nominally the same) multilayer sample was prepared (sample $4 \times 50B$) but it was not covered by the electrode structure.

The THz time-domain spectroscopy was used to determine the complex permittivity spectra at various temperatures with and without the electric bias. Experiments without bias were carried out on the part of the sample $4 \times 50A$ not covered with electrodes in order to characterize the zero-field permittivity and loss spectra of the STO layers. As pointed out earlier, the accuracy of the determination of the permittivity of thin films is usually rather low.[20] In addition, in order to limit the probing THz beam to the bare part of the sample, an aperture of 3 mm was used in THz transmission experiments; this may lead to diffraction effects and the low-frequency part of the THz spectra (which was subsequently found to be very important for the interpretation) may suffer from larger systematic errors, especially if the sample is handled in the cryostat (problems arise with precise positioning of the sample and reference). For this reason, the sample $4 \times 50B$ was prepared following the same experimental protocol and the temperature-dependent zero-bias THz transmission experiments were carried out with this sample by using an aperture of 6 mm. In addition, careful preliminary measurements of the substrate thickness, as described in Ref. [17], were performed with both samples in order to reach a high accuracy.

The experiments without bias consisted of two consecutive measurements for each temperature: one of a signal wave form $E_s(t)$, using a sample with the thin-film structure, and one of a reference wave form $E_r(t)$ with a bare DSO substrate. The ratio of the Fourier transforms of the time-domain wave forms provided the complex THz transmittance spectrum of the film $t(\omega) = E_s(\omega)/E_r(\omega)$. The permittivity of the STO film was then retrieved by using the appropriate formula for the thin-film transmittance [see Eq. (3) in Ref. [17]].

The electric field-induced changes in the complex dielectric spectra were subsequently determined by measurements of the THz transmission through the part of the sample $4 \times 50A$ provided with electrodes and with an applied bias. We used polarized THz pulses with their electric field parallel to the applied bias field, i.e., perpendicular to the electrode fingers: in this geometry, the electrode structure is transparent to the THz radiation. Here the reference THz wave forms $E_0(t)$ were measured with the electric field off and the signal wave forms $E_V(t)$ were obtained with the applied dc bias; the field-induced changes in the permittivity were then retrieved from the complex transmission function $t'(\omega) = E_V(\omega)/E_0(\omega)$.[17]

III. EXPERIMENTAL RESULTS AND EVALUATION

Figure 1 shows examples of THz complex dielectric spectra of unbiased samples. Both the real and imaginary parts of the permittivity decrease with a decreasing temperature. This could be related to a hardening of the soft-mode frequency below the ferroelectric phase transition, which would then occur close to the room temperature. This hypothesis will be proven below by fitting the experimental data with our model.
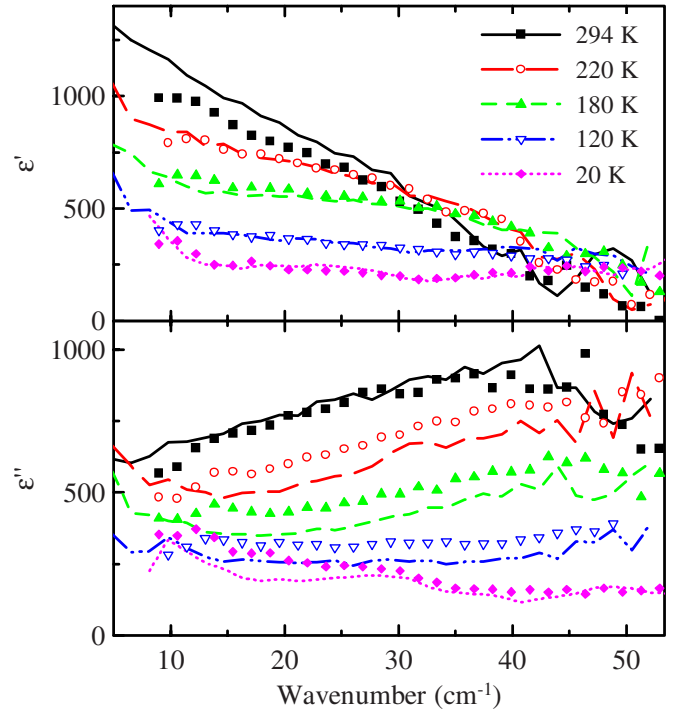

FIG. 1. (Color online) Complex permittivity spectra (without bias) of samples $4 \times 50A$ (symbols) and $4 \times 50B$ (lines) as a function of temperature.

We found a very good agreement between the experimental data obtained with the two investigated samples. This statement and the data plotted in Fig. 1 require a more detailed discussion. As pointed out in Ref. [17], the systematic experimental error in the determination of THz dielectric spectra in thin films is mostly related to the accuracy of the determination of the substrate thickness due to the so-called phase error. We performed a very careful evaluation of the substrate thickness prior to the thin-film deposition by means of the THz time-domain spectroscopy of the bare substrates.[17,21] Nevertheless, small errors on the order of 200 nm cannot be avoided. In our case, when the bare substrate used for the reference measurement and the substrate with thin-film multilayer have approximately the same thickness, the leading term describing the error in the refractive index Δn of the thin film reads as

$$\Delta n \approx n_s \frac{\Delta d_s}{d}, \tag{1}$$

where d is the film thickness, Δd_s is the error in the substrate thickness determination, and n_s is the refractive index of the substrate. In this way, an error in the substrate thickness determination of 100 nm corresponds to $\Delta n \approx 2$; the error in the absorptive index $\Delta \kappa$ is much smaller. Such an offset is then responsible for a systematic error in the measured complex permittivity $\varepsilon = \varepsilon' + i\varepsilon''$, which can be expressed using the formula

$$\varepsilon_{\text{new}} = (\sqrt{\varepsilon} - \Delta n)^2. \tag{2}$$

In order to be able to compare easily the data measured on the samples $4 \times 50A$ and $4 \times 50B$, we transformed the per-
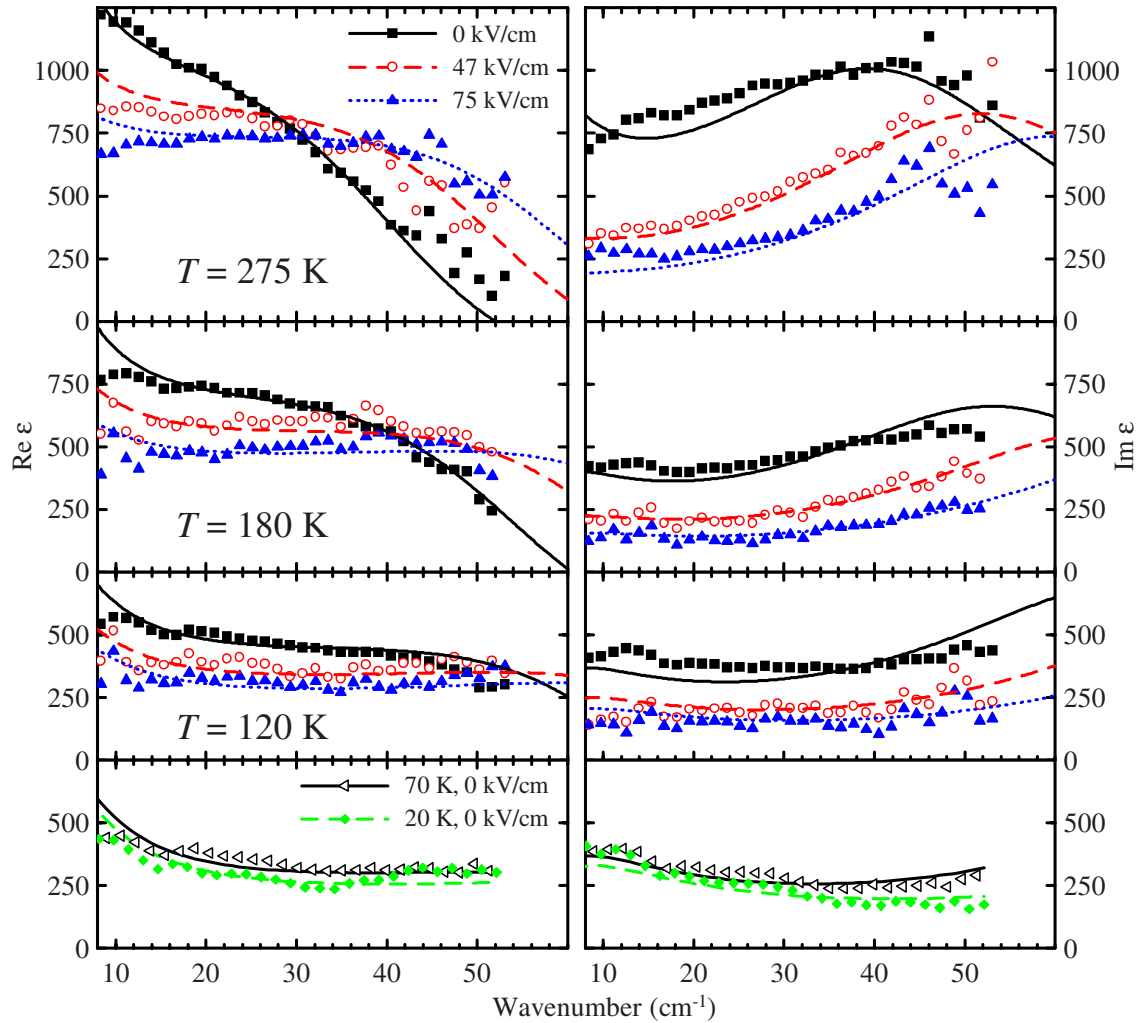
FIG. 2. (Color online) Complex THz spectra for sample $4 \times 50A$ for several temperatures and bias field. Symbols: experimental data; lines: fit with Eq. (4).

mittivity of the sample $4 \times 50A$ using Eq. (2) with a trial value of $\Delta n = 2$. This transformation corresponds to a decrease in ε' by about 70–140 and of ε'' roughly by 30–70. Having performed this transformation, we obtained a good agreement between the two samples. This proves an excellent reproducibility in the thin-film elaboration process and demonstrates the state-of-the-art accuracy in our THz measurements. Note, however, that the only reason why we show the transformed data in Fig. 1 is to allow an easy comparison: due to the lack of knowledge of Δd, it is not possible to remove the systematic error in ε in this way. All the fits presented in the next section were performed with the as-measured data.

IV. DISCUSSION

Figure 2 displays the complex dielectric spectra of sample $4 \times 50A$ as a function of the electric bias for several temperatures. Applying the electric field leads to a hardening of the soft mode as clearly observed in spectra obtained at higher temperatures. In contrast, the tunability of the permittivity is found to be substantially smaller at low temperatures, where

the soft-mode frequency is higher even without bias. It has been pointed out previously[7,17] that a low-frequency excitation (at $\gamma \approx 10$ cm^{-1}) of relaxation type is observed in the room-temperature spectra. This excitation was shown to be silent, i.e., not directly coupled to the polarization; however, it was linearly coupled to the soft mode (modeled as a damped oscillator with a bare eigenfrequency ω_0, damping Γ, and oscillator strength f) with a coupling constant $\delta \approx 35$ cm^{-1}. The experimental spectra of different STO/DSO multilayers at room temperature were successfully fitted with[17]

$$\varepsilon(\omega) = \frac{f(1 - i\omega/\gamma)}{(\omega_0^2 - \omega^2 - i\omega\Gamma)(1 - i\omega/\gamma) - \delta^2} + \varepsilon_\infty. \quad (3)$$

Within this model, the appearance and strength of the relaxation mode in the THz dielectric spectra are essentially related to the soft-mode frequency: one finds that the fingerprint of the relaxation practically should not be observed for high soft phonon frequency values ($\omega_0 \gtrsim 90$ cm^{-1}), while it should dominate the spectra when the soft-mode frequency is low ($\omega_0 \approx 40$ cm^{-1}). We point out that the spectra shown in
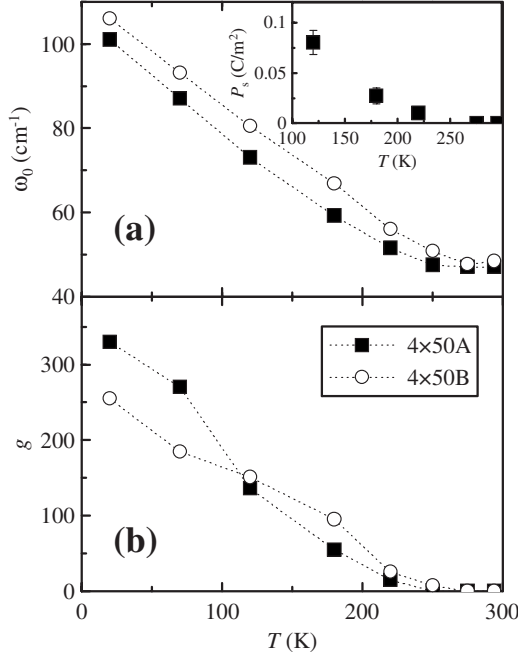
FIG. 3. Temperature dependence of the (a) soft-mode frequency and (b) relaxation strength for both samples studied. Inset: estimation of the temperature dependence of the spontaneous polarization.

FIG. 4. (Color online) Soft-mode eigenfrequency as a function of the electric bias at several temperatures for sample 4×50A. Symbols: experiment; lines: fit with Eq. (8), yielding P_s. Crosses represent an estimation after room-temperature measurements at 10 GHz of a 50-nm-thick STO/DSO in Ref. 12.

Figs. 1 and 2 strongly suggest that this statement is no more valid at low temperatures, where apparently the soft-mode frequency is high while the fingerprints of the relaxation mode are still clearly observed.

Taking into account these facts, we decided to employ a more general formula,[22,23] which assumes that the bare relaxational mode contributes directly to the permittivity

$$\varepsilon(\omega) = \frac{f(1 - i\omega/\gamma) + g(\omega_0^2 - \omega^2 - i\omega\Gamma) \pm 2\delta\sqrt{fg}}{(\omega_0^2 - \omega^2 - i\omega\Gamma)(1 - i\omega/\gamma) - \delta^2} + \varepsilon_\infty. \tag{4}$$

The relaxation mode strength g is proportional to the squared effective charge of the mode. The fits show that it vanishes in the paraelectric phase (as observed in Ref. 17), while it is nonzero in the ferroelectric one and it grows as the temperature decreases below the transition temperature. The sign in the numerator of Eq. (4) describes whether the effective charge of the two modes has the same ($-$) or opposite ($+$) sign.

All the spectra measured with and without bias were fitted by the model (4). We performed a global fit, where we assumed that Γ, f, γ, and δ are known from the room-temperature data[17] and that they are temperature and field independent; $g(T)$ was then supposed to be temperature dependent and field independent[24] and the soft-mode frequency $\omega_0(T, E)$ was allowed to be fitted independently for each spectrum. Examples of fits for some spectra are displayed in Fig. 2. More than 50 complex spectra were simultaneously fitted by using the procedure described above; the formula (4) with the sign "$+$" was found to fit the experimental data
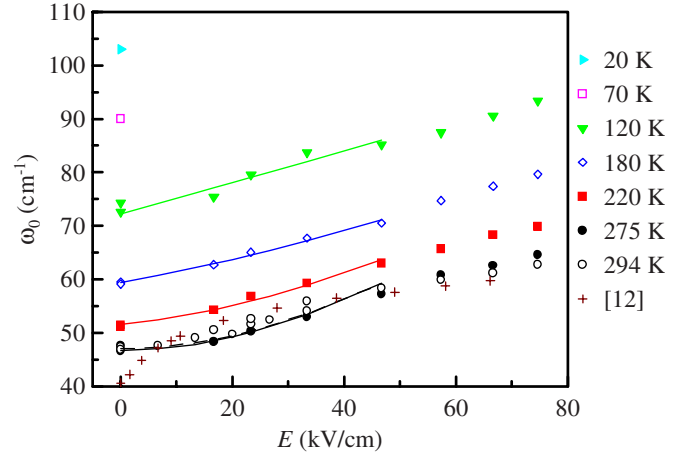
quite satisfactorily. This sign corresponds to opposite effective charges of the soft and central modes and implies a destructive interference in the spectral range between the resonance frequencies of the two modes.

The soft-mode frequency without bias and the relaxation strength as a function of temperature are shown in Fig. 3 for both samples. From the data plotted in Fig. 3, the ferroelectric transition temperature appears to occur slightly below the room temperature, say, between 250 and 275 K.

In Fig. 4, we show the electric field tunability of the soft mode at various temperatures as obtained from the fit (measurements with bias were not done at 70 and 20 K). It appears that the soft mode significantly hardens when the temperature is decreased but at the same time the tunability in terms of the field-induced change in the soft-mode frequency remains surprisingly high even at low temperatures. To interpret the soft-mode behavior, we consider the simplest form of the Helmholtz free-energy expansion F

$$F = \frac{\omega_a^2}{2f\varepsilon_{\mathrm{vac}}}P^2 + \frac{\beta}{4}P^4, \tag{5}$$

where $\varepsilon_{\mathrm{vac}}$ is the vacuum permittivity and the coefficient β characterizes the anharmonicity of the soft-mode potential minimum. We denote by $\omega_0(T, E)$ the value of the soft-mode eigenfrequency at a given temperature and electric bias. This quantity was not measured in the paraelectric phase above room temperature; nevertheless, following Eq. (5), we formally obtain $\omega_0(T, 0) = \omega_a(T)$ in this phase. In the ferroelectric phase, ω_a^2 is renormalized due to the nonvanishing spontaneous polarization P_s; the value $\omega_0(T, 0)$ was experimentally obtained in this phase. In our THz experiments with an applied bias E, we deal with three polarization components, the dc (or low-frequency) ones P_s, $\Delta P(E)$ (field-induced), and a weak dynamic one P_{THz} oscillating at THz frequencies as the response to the probing pulse. The total in-plane polarization then reads as

$$P = P_s + \Delta P(E) + P_{\text{THz}}. \tag{6}$$

The harmonic part of the free energy (5), oscillating at THz frequencies, then takes the form

$$F_{\text{THz}} = \frac{\omega_a^2}{2 f \varepsilon_{\text{vac}}} P_{\text{THz}}^2 + \frac{3}{2} \beta [P_s + \Delta P(E)]^2 P_{\text{THz}}^2. \tag{7}$$

Note that thanks to our interdigitated structure, we apply relatively high electric fields which may pole the sample and create regions (in the gaps between electrode fingers) with a

nonvanishing macroscopic spontaneous polarization. Owing to the interdigitated character of the electrodes, the adjacent regions are poled with opposite field, i.e., the sign of P_s alternates in adjacent electrode gaps (e.g., positive in odd gaps and negative in even gaps between electrode fingers). Note also, however, that the sign of P_s and $\Delta P(E)$ is always the same regardless the orientation of the field. Hence, the mixed term $P_s \cdot \Delta P(E)$ in Eq. (7) is positive in the whole probed part of the sample and contributes to the electric field-induced soft-mode frequency renormalization

$$\omega_0(T,E) \approx \omega_0(T,0) \sqrt{1 + 3\beta [\varepsilon_{\text{vac}} f / \omega_0^2(T,0)]^3 E^2 + 6\beta [\varepsilon_{\text{vac}} f / \omega_0^2(T,0)]^2 P_s E}. \tag{8}$$

The last term under the square root is absent in the paraelectric phase[17] and in an unpoled sample, while it may significantly contribute to the soft-mode tunability at low temperatures. The best fits of the field dependence of the soft-mode frequency at several temperatures are shown in Fig. 4; the fits were calculated assuming that β is temperature independent and P_s was a fitting parameter at each temperature. The values of the spontaneous polarization as estimated from the fits are shown in the inset of Fig. 3.

At room temperature, P_s vanishes and, in the weak-field limit ($E < 35$ kV/cm), the soft-mode frequency displays a quadratic growth with the external bias (Fig. 4). The field-induced dc polarization grows up to $\Delta P \approx 0.04$ C/m² at $E \approx 35$ kV/cm.

Thin STO films grown on YBCO substrates were found to be ferroelectric below 90 K with a spontaneous polarization of $P_s \approx 0.3$ C/m² at helium temperatures.[25] This value is also comparable to the saturated one found in the ferroelectric phase of BaTiO₃ single crystals.[26] Taking into account these facts, we think that a value of $P_s \approx 0.08$ C/m² at 120 K (Fig. 3) stemming from our data is quite reasonable. Nevertheless, this value should be taken with caution as possible contribution of higher-order terms cannot be excluded within the accuracy of our experimental data.

In Ref. 17, a comparison of the soft-mode properties (including the anharmonic coefficient β) has been made for a set of strained samples with different thicknesses of STO layers. These data were obtained by THz time-domain measurements. It seems then useful to make a comparison of the THz data, which essentially characterize the soft-mode contribution to the static permittivity with the microwave ones in order to determine whether some additional contribution appears below the phonon range. However, this seems to be difficult with the currently available experimental results, as there is no report characterizing a single sample in both GHz and THz ranges. Here we provide a semiquantitative attempt to estimate this difference by comparison of a single 50-nm-thick STO layer grown on DSO and characterized in the GHz range[12] with our multilayer sample (similar comparison can be performed with any of the samples investigated in Ref. 17). A direct comparison is impossible, as the estimated val-

ues of the static permittivity from the GHz data ($\sim$5800) (ref. 12) and from the THz data ($\sim$2350) (Ref. 17) substantially differ and, consequently, the tunability curves of the dielectric constant are quite different as well. It is not possible to assess whether this difference comes from an additional GHz contribution or simply from the fact that the samples (and in-plane strains) are different.

An indirect comparison can be made starting from an assumption of the validity of our soft-mode model down to the GHz frequency range. It is then possible to estimate the variation in the soft-mode eigenfrequency from the room-temperature tuning curve shown in Fig. 3 in Ref. 12 by using Eq. (4) in the static limit ($\omega \to 0$) and with $\delta = 35$ cm⁻¹, $f = 2.3 \times 10^6$ cm⁻², and $g = 0$; this is shown in Fig. 4. We observe that for fields higher than $\sim$7 kV/cm, a relatively good agreement with the THz data is obtained. However, the resulting curve presents a clearly nonquadratic behavior (dip) close to zero bias. This feature can be interpreted as an artifact of our estimation within the soft-mode model and could be attributed to an additional GHz contribution to the permittivity. A strong contribution to the permittivity in the GHz range, which was suppressed upon temperature annealing, has been also reported in STO films studied in Ref. 14. Deeper understanding can be obtained only if concerted experiments in GHz and THz ranges are carried out.

V. CONCLUSION

We determined temperature and electric field dependence of the dielectric permittivity in the THz range of strained SrTiO₃/DyScO₃ multilayers. The ferroelectric phase sets in around 270 K. A general model consisting of a coupled soft mode with a central mode is able to describe all the measured spectra. The effective charge in the central mode has to be taken into account in the ferroelectric phase and is found to be opposite to that of the soft mode. The variation in the soft-mode frequency with temperature and electric field is found to be the key quantity for the overall behavior of THz dielectric spectra. The electric field tunability of the soft

mode decreases with decreasing temperature in the ferroelectric phase; however, this decrease is considerably slowed down by a high value of the spontaneous polarization, which renormalizes the effective soft-mode potential. Direct measurements of the spontaneous polarization in the strained samples then would be very helpful in order to confirm the proposed quantitative picture of the soft-mode behavior.

*Author to whom correspondence should be addressed; kuzelp@fzu.cz

[1] P. Kužel and F. Kadlec, C. R. Phys. **9**, 197 (2008).

[2] R. Piesiewicz, T. Kleine-Ostmann, N. Krumbholz, D. Mittleman, M. Koch, J. Schoebel, and T. Kurner, IEEE Antennas Propag. Mag. **49**, 24 (2007).

[3] H.-T. Chen, W. J. Padilla, J. M. O. Zide, A. C. Gossard, A. J. Taylor, and R. D. Averitt, Nature (London) **444**, 597 (2006).

[4] H.-T. Chen, W. J. Padilla, J. M. O. Zide, S. R. Bank, A. C. Gossard, A. J. Taylor, and R. D. Averitt, Opt. Lett. **32**, 1620 (2007).

[5] H.-T. Chen, J. F. O'Hara, A. K. Azad, A. J. Taylor, R. D. Averitt, D. B. Shrekenhamer, and W. J. Padilla, Nat. Photonics **2**, 295 (2008).

[6] L. Fekete, F. Kadlec, P. Kužel, and H. Němec, Opt. Lett. **32**, 680 (2007).

[7] P. Kužel, C. Kadlec, F. Kadlec, J. Schubert, and G. Panaitov, Appl. Phys. Lett. **93**, 052910 (2008).

[8] Q. Zhao, L. Kang, B. Du, H. Zhao, Q. Xie, X. Huang, B. Li, J. Zhou, and L. Li, Phys. Rev. Lett. **101**, 027402 (2008).

[9] H. Němec, P. Kužel, F. Kadlec, C. Kadlec, R. Yahiaoui, and P. Mounaix, Phys. Rev. B **79**, 241108(R) (2009).

[10] M. E. Lines and A. M. Glass, *Principles and Applications of Ferroelectrics and Related Materials* (Clarendon, Oxford, 1979).

[11] K. A. Müller and H. Burkard, Phys. Rev. B **19**, 3593 (1979).

[12] J. H. Haeni, P. Irvin, W. Chang, R. Uecker, P. Reiche, Y. L. Li, S. Choudhury, W. Tian, M. E. Hawley, B. Craigo, A. K. Tagantsev, X. Q. Pan, S. K. Streiffer, L. Q. Chen, S. W. Kirchoefer, J. Levy, and D. G. Schlom, Nature (London) **430**, 758 (2004).

[13] P. Irvin, J. Levy, J. H. Haeni, and D. G. Schlom, Appl. Phys. Lett. **88**, 042902 (2006).

[14] W. Chang, J. A. Bellotti, S. W. Kirchoefer, and J. M. Pond, J. Electroceram. **17**, 487 (2006).

[15] P. Kužel, F. Kadlec, H. Němec, R. Ott, E. Hollmann, and N. Klein, Appl. Phys. Lett. **88**, 102901 (2006).

[16] P. Kužel, F. Kadlec, J. Petzelt, J. Schubert, and G. Panaitov, Appl. Phys. Lett. **91**, 232911 (2007).

[17] C. Kadlec, F. Kadlec, H. Němec, P. Kužel, J. Schubert, and G. Panaitov, J. Phys.: Condens. Matter **21**, 115902 (2009).

[18] I. Ponomareva, L. Bellaiche, T. Ostapchuk, J. Hlinka, and J. Petzelt, Phys. Rev. B **77**, 012102 (2008).

[19] J. Hlinka, T. Ostapchuk, D. Nuzhnyy, J. Petzelt, P. Kužel, C. Kadlec, P. Vaněk, I. Ponomareva, and L. Bellaiche, Phys. Rev. Lett. **101**, 167402 (2008).

[20] J. Petzelt, P. Kužel, I. Rychetský, A. Pashkin, and T. Ostapchuk, Ferroelectrics **288**, 169 (2003).

[21] L. Duvillaret, F. Garet, and J.-L. Coutaz, IEEE J. Sel. Top. Quantum Electron. **2**, 739 (1996).

[22] A. S. Barker, Jr., and J. J. Hopfield, Phys. Rev. **135**, A1732 (1964).

[23] Y. Girshberg and Y. Yacoby, Solid State Commun. **103**, 425 (1997).

[24] Our experimental data are not sufficiently precise to determine unambiguously a possible field-induced variation in g from the fits. Nevertheless, we observed a small general tendency of this parameter to decrease with increasing field at low temperatures.

[25] D. Fuchs, C. W. Schneider, R. Schneider, and H. Rietschel, J. Appl. Phys. **85**, 7362 (1999).

[26] W. J. Merz, Phys. Rev. **91**, 513 (1953).